Supplementary Material (ESI) for New Journal of Chemistry
This journal is © The Royal Society of Chemistry and
The Centre National de la Recherche Scientifique, 2009

Supporting information

Solvent-Sensitive Charge-Transfer Absorption Behaviours and Dual-Emissive Fluorescent Property of a Thiazole-Conjugated Pyridinium Complex

Zhan-Xian Li,[a,b] Chun-Hu Xu,[a] Wei Sun,[a] Yan-Chun Bai,[a] Chao Zhang,[a] Chen-Jie Fang,[a] and Chun-Hua Yan* [a]

[a] Beijing National Laboratory for Molecular Sciences, State Key Laboratory of Rare Earth Materials Chemistry and Applications, PKU-HKU Joint Laboratory in Rare Earth Materials and Bioinorganic Chemistry, Peking University, Beijing 100871, China. Fax: +86-10-6275-4179, E-mail: yan@pku.edu.cn

[b] Laboratory of Functional Materials, Department of Chemistry, Zhengzhou University, Zhengzhou 450001, China.

1. Absorption spectra

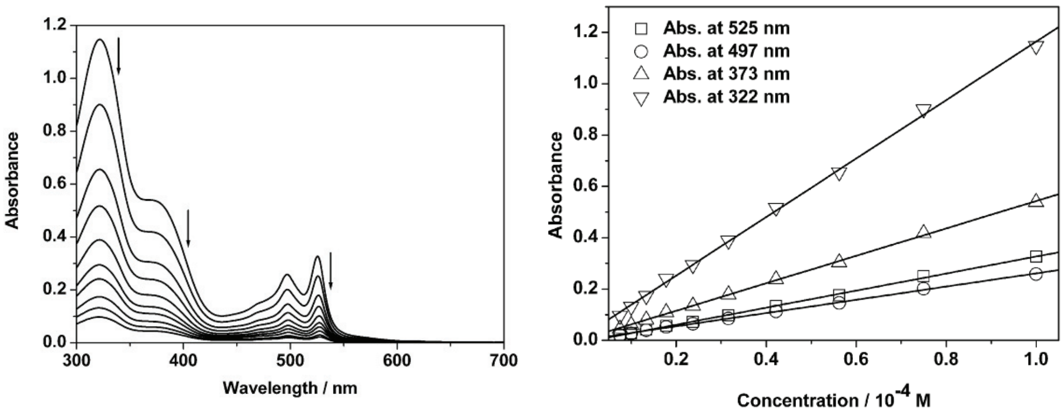

A

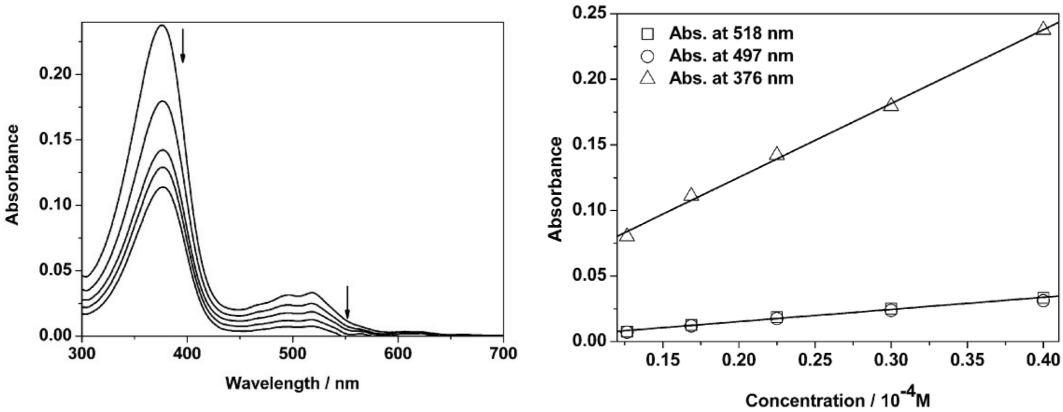

B

Fig. S1 Changes of absorption spectra of **4-MeB** (left) and absorbance changes at the specific wavelength (right) in 1,4-dioxane (A) and EtOAc (B) with the concentration decreased. Solid lines in the right of Fig. (A) and (B) represent fit lines of the absorbance at specific wavelength to the concentration of **4-MeB**. The concentration of **4-MeB** changes from 1.0×10^{-4} mol·L^{-1} to 8.6×10^{-6} mol·L^{-1} in 1,4-dioxane and from 4.0×10^{-5} to 1.9×10^{-5} mol·L^{-1} in EtOAc.

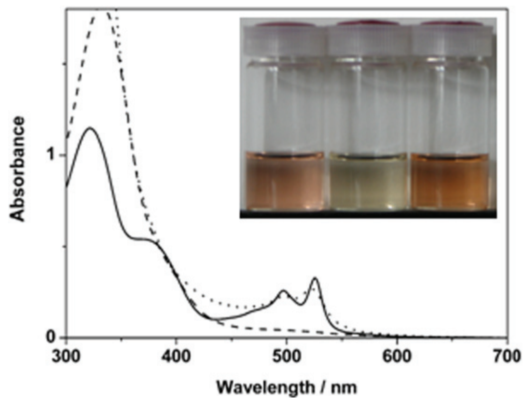

Fig. S2 Absorption spectra of **4-MeB** in 1,4-dioxane (c = 1.0×10^{-4} mol·L^{-1}) (solid line: **4-MeB** only; dash line: **4-MeB** with $AgPF_6$ added; dot line: **4-MeB** with $AgPF_6$ and (n-Bu)$_4$NBr added sequentially). Insert: color changes of **4-MeB** in 1,4-dioxane (from left to right: **4-MeB** only; **4-MeB** with $AgPF_6$ added; **4-MeB** with $AgPF_6$ and (*n*-Bu)$_4$NBr added sequentially).

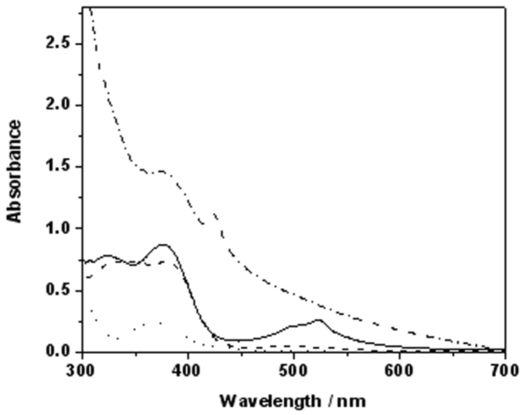

Fig. S3 Absorption spectra of **4-MeB** in THF (c = 1.2×10^{-4} mol·L^{-1}) (solid line: **4-MeB** only; dash line: **4-MeB** with $AgPF_6$ added; dot line: (*n*-Bu)$_4$NI only**;** dash dot: **4-MeB** with $AgPF_6$ and (*n*-Bu)$_4$NI added sequentially).

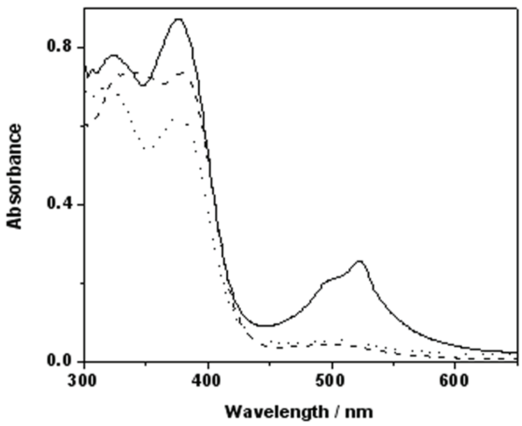

Fig. S4 Absorption spectra of **4-MeB** in THF (c = 1.2×10^{-4} mol·L^{-1}) (solid line: **4-MeB** only; dash line: **4-MeB** with $AgPF_6$ added; dot line: **4-MeB** with $AgPF_6$ and Me_4NCl added sequentially).

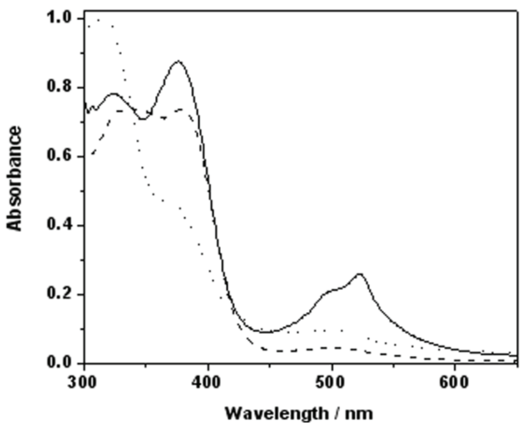

Fig. S5 Absorption spectra of **4-MeB** in THF (c = 1.2×10^{-4} mol·L^{-1}) (solid line: **4-MeB** only; dash line: **4-MeB** with $AgPF_6$ added; dot line: **4-MeB** with $AgPF_6$ and Et_3N added sequentially).

2. Theoretical calculation results

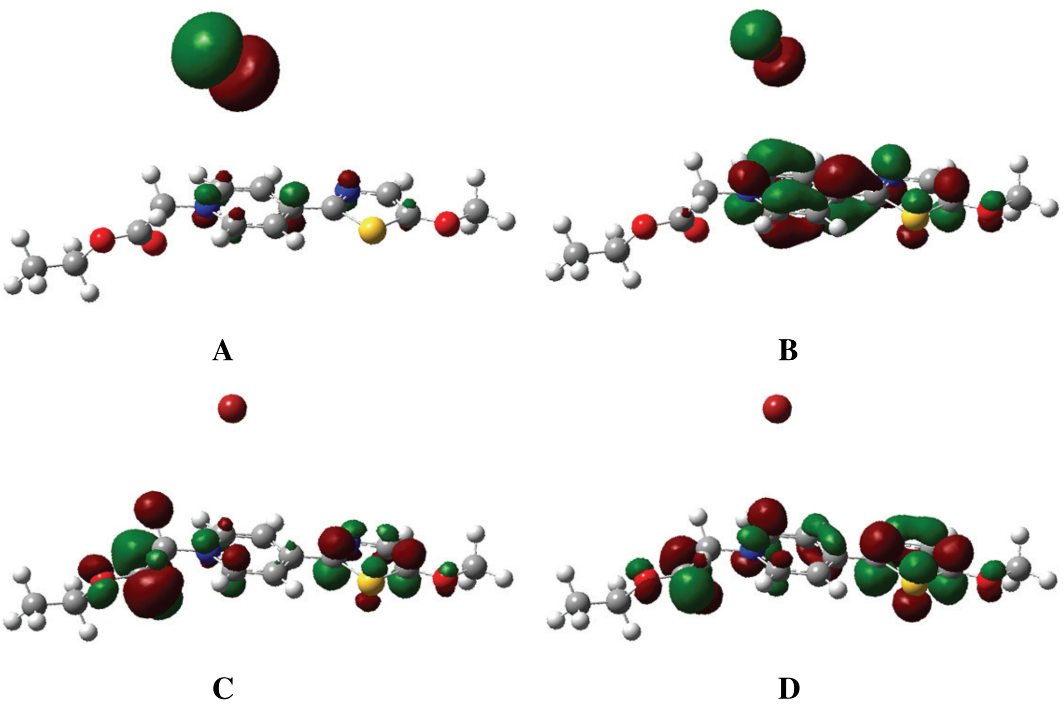

Fig. S6 HOMO (A), LUMO (B), LUMO+2 (C), and LUMO+3 (D) of **4-MeB** calculated at the MPW1PW91/3-21G level by Gaussian 03 while the distance between bromide anion and nitrogen atom of pyridyl ring is set as 5.40 Å.

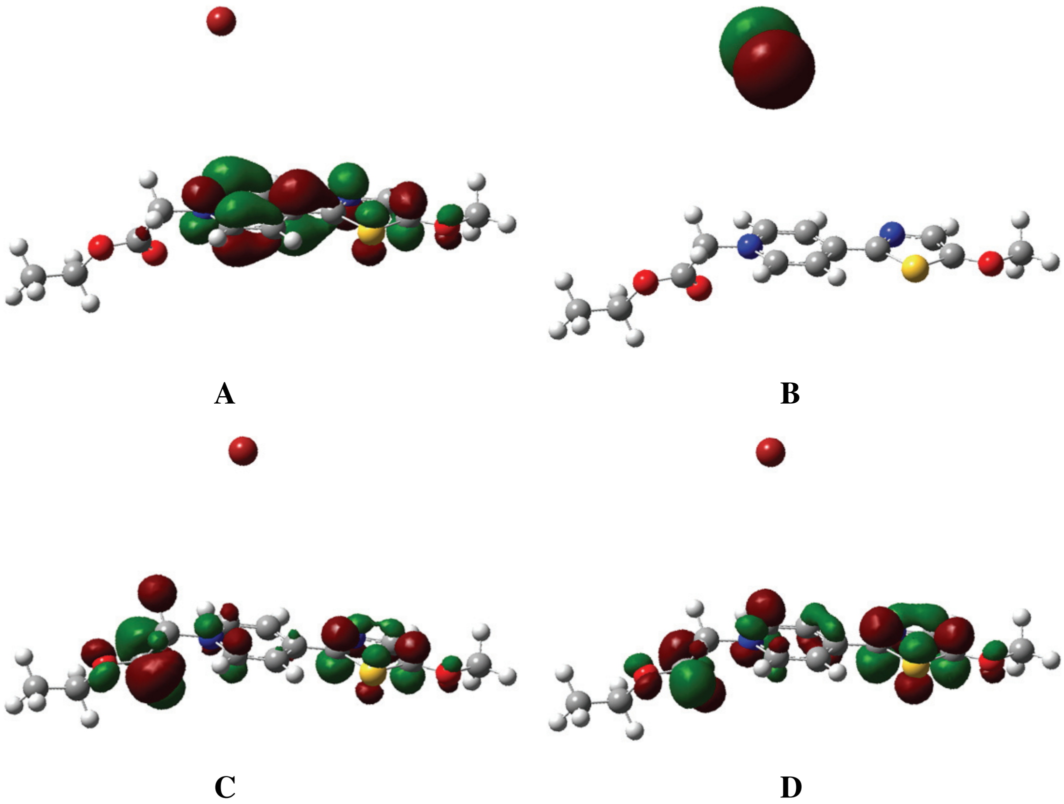

Fig. S7 HOMO (A), LUMO (B), LUMO+2 (C), and LUMO+3 (D) of **4-MeB** calculated at the MPW1PW91/3-21G level by Gaussian 03 while the distance between bromide anion and nitrogen atom of pyridyl ring is set as 6.75 Å.

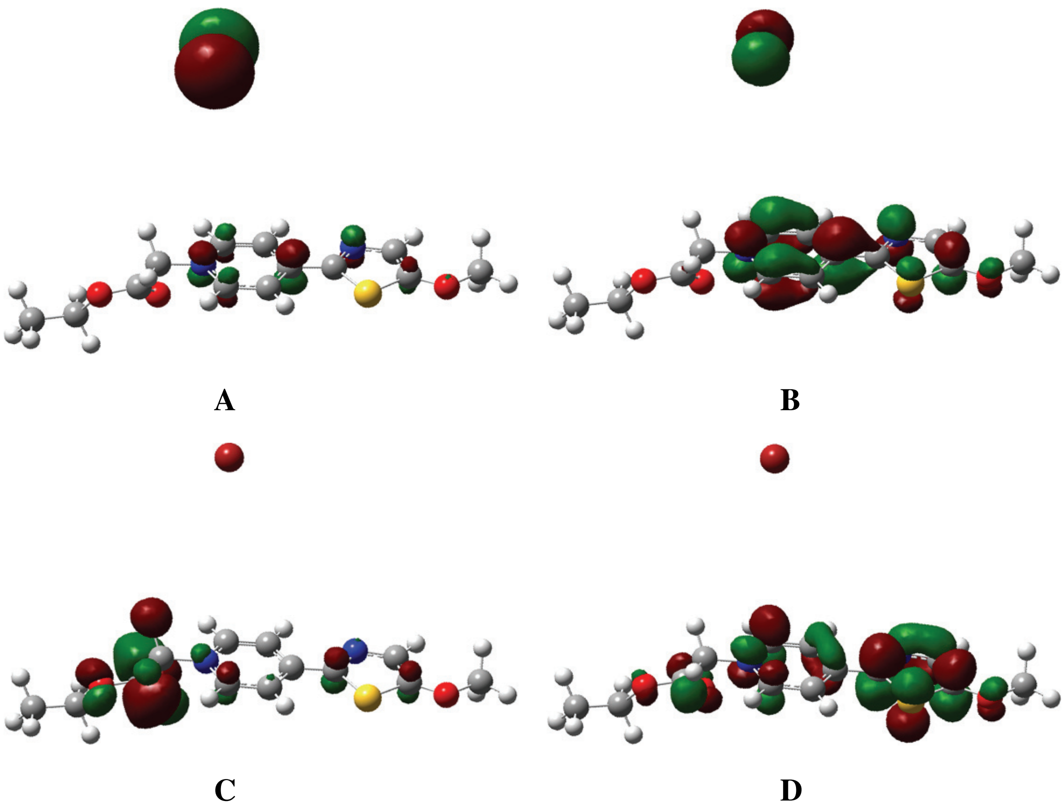

Fig. S8 HOMO (A), LUMO (B), LUMO+2 (C), and LUMO+3 (D) of **4-MeB** calculated at the MPW1PW91/3-21G level by Gaussian 03 while the distance between bromide anion and nitrogen atom of pyridyl ring is set as 8.10 Å.

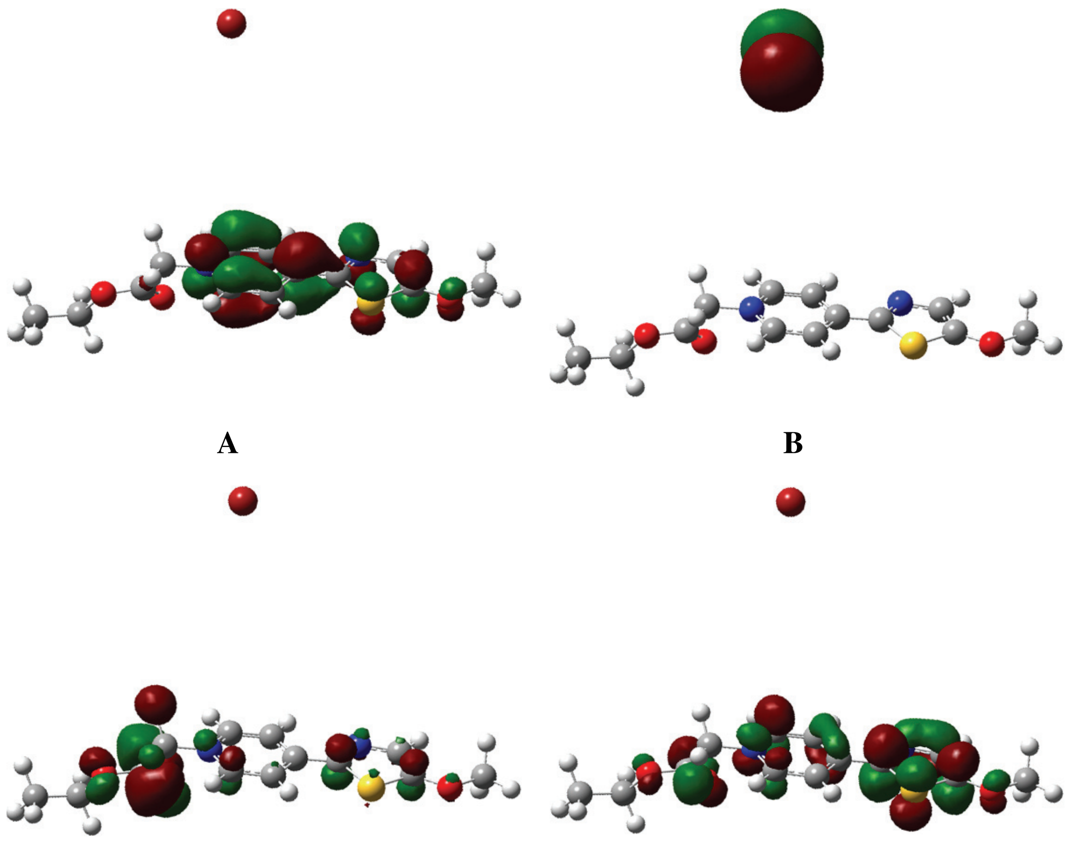

C D

Fig. S9 HOMO (A), LUMO (B), LUMO+2 (C), and LUMO+3 (D) of **4-MeB** calculated at the MPW1PW91/3-21G level by Gaussian 03 while the distance between bromide anion and nitrogen atom of pyridyl ring is set as 9.45 Å.

3. Fluorescence emission and excitation spectra

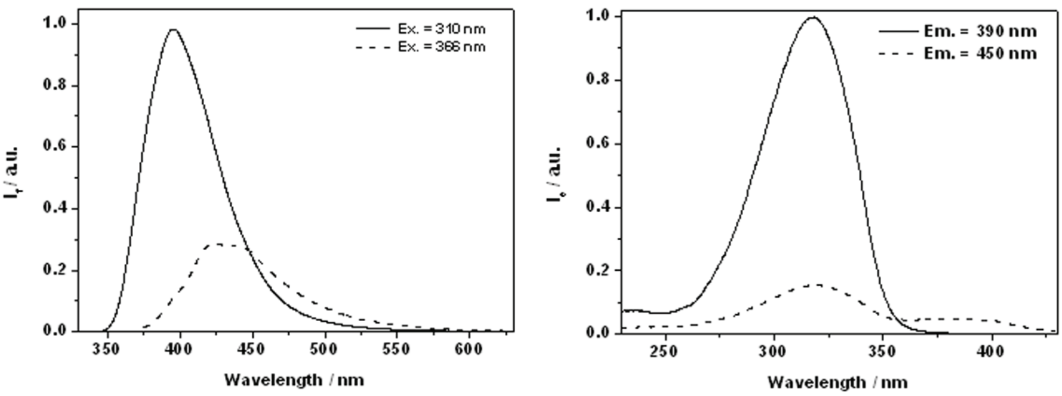

A B

Fig. S10 Emission spectra of **4-MeB** in 1,4-dioxane upon excitation at 310 and 366 nm (A); excitation spectra of **4-MeB** in 1,4-dioxane at emission wavelength of 390 and 450 nm (B).

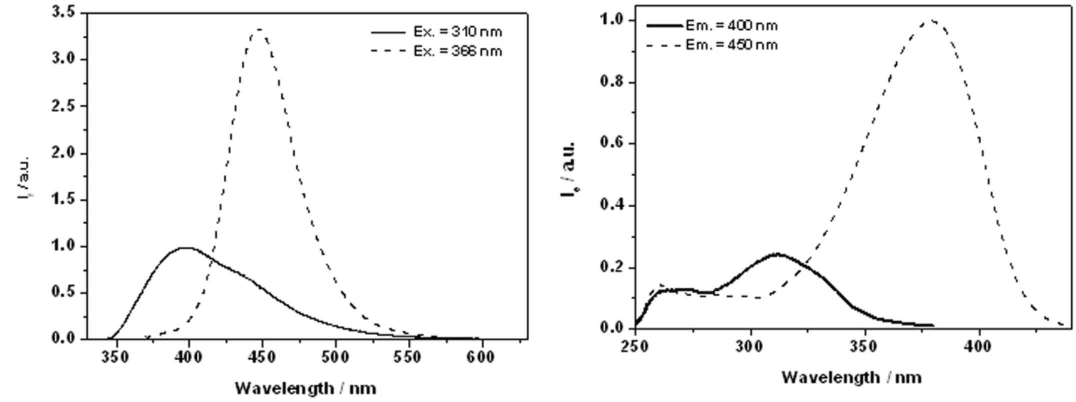

A B

Fig. S11 Emission spectra of **4-MeB** in EtOAc upon excitation at 310 and 366 nm (A); excitation spectra of **4-MeB** in EtOAc at emission wavelength of 400 and 450 nm (B).

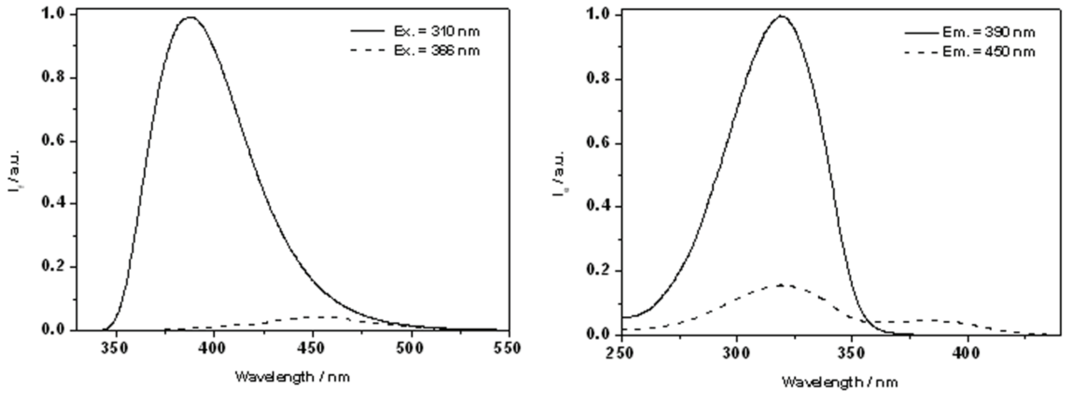

A B

Fig. S12 Emission spectra of **4-MeB** in THF upon excitation at 310 and 366 nm (A); excitation spectra of **4-MeB** in THF at emission wavelength of 390 and 450 nm (B).

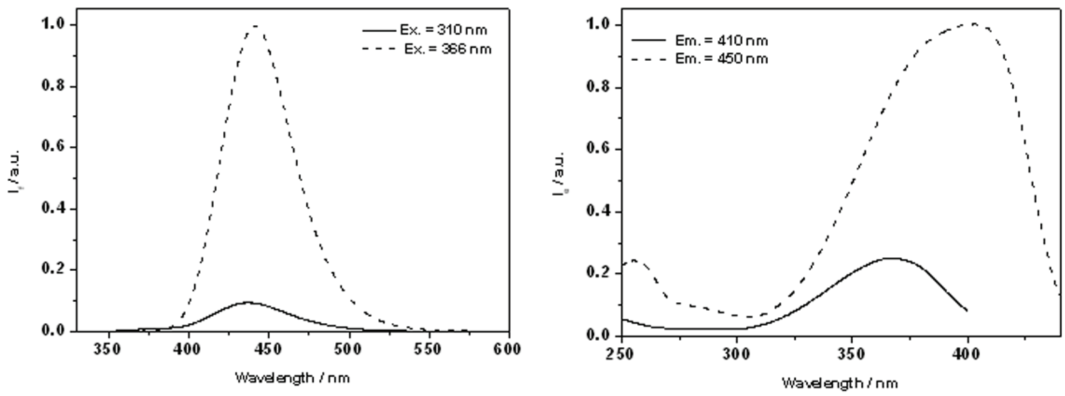

A B

Fig. S13 Emission spectra of **4-MeB** in DCM upon excitation at 310 and 366 nm (A); excitation spectra of **4-MeB** in DCM at emission wavelength of 410 and 450 nm (B).

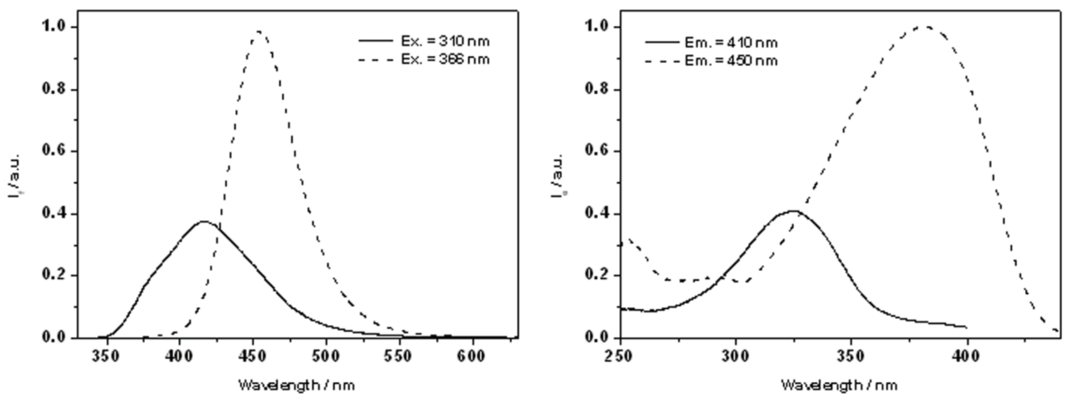

A **B**

Fig. S14 Emission spectra of **4-MeB** in methanol upon excitation at 310 and 366 nm (A); excitation spectra of **4-MeB** in methanol at emission wavelength of 410 and 450 nm (B).

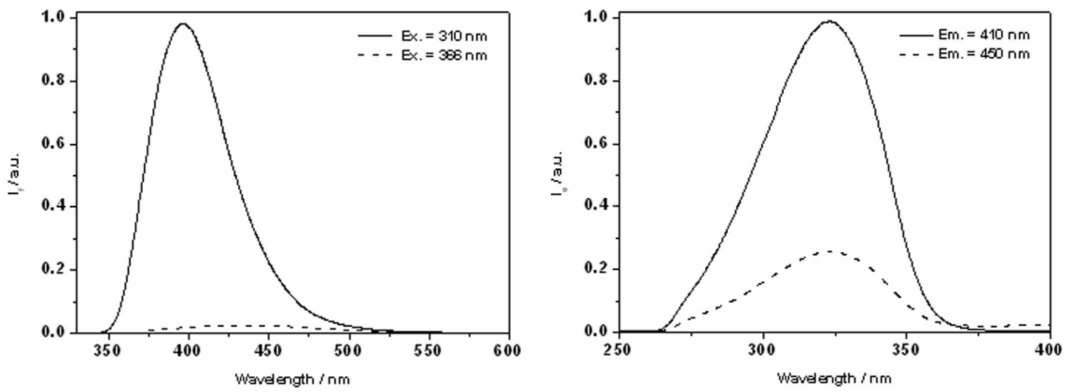

A **B**

Fig. S15 Emission spectra of **4-MeB** in DMF upon excitation at 310 and 366 nm (A); excitation spectra of **4-MeB** in DMF at emission wavelength of 410 and 450 nm (B).

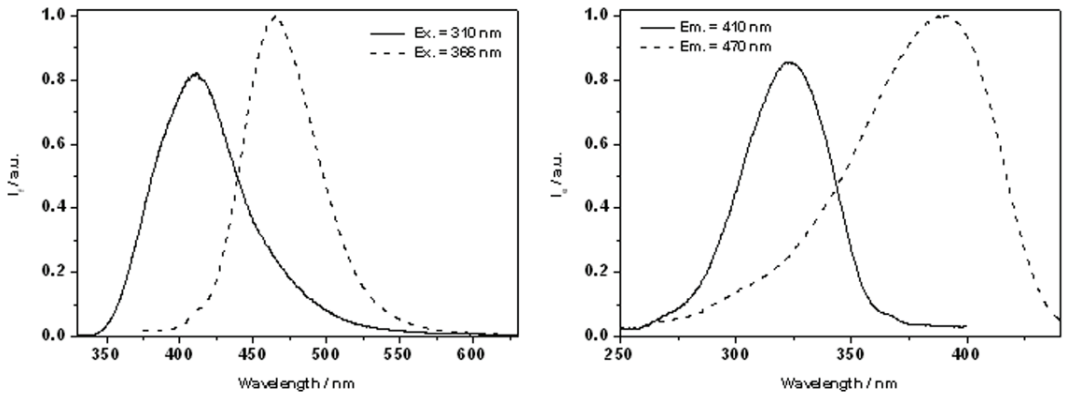

A **B**

Fig. S16 Emission spectra of **4-MeB** in DMSO upon excitation at 310 and 366 nm (A); excitation spectra of **4-MeB** in DMSO at emission wavelength of 410 and 470 nm (B).

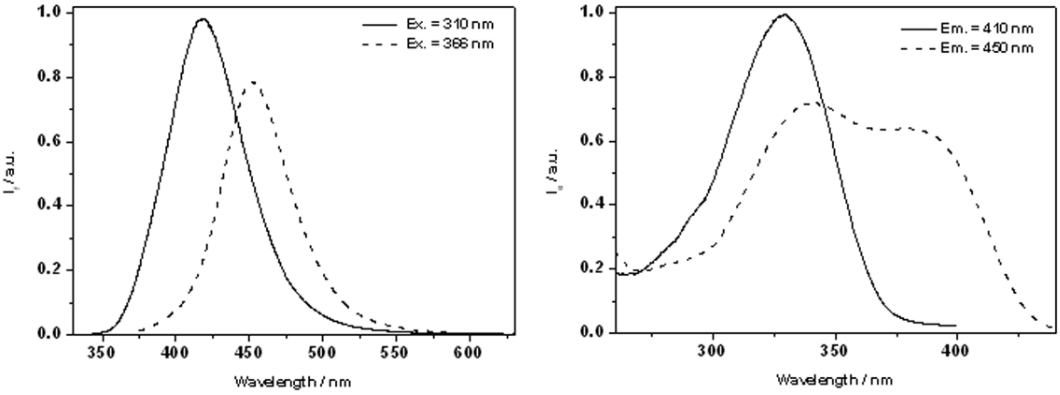

A B

Fig. S17 Emission spectra of **4-MeB** in water upon excitation at 310 and 366 nm (A); excitation spectra of **4-MeB** in DMSO at emission wavelength of 410 and 450 nm (B).

4. Radiative decay curves

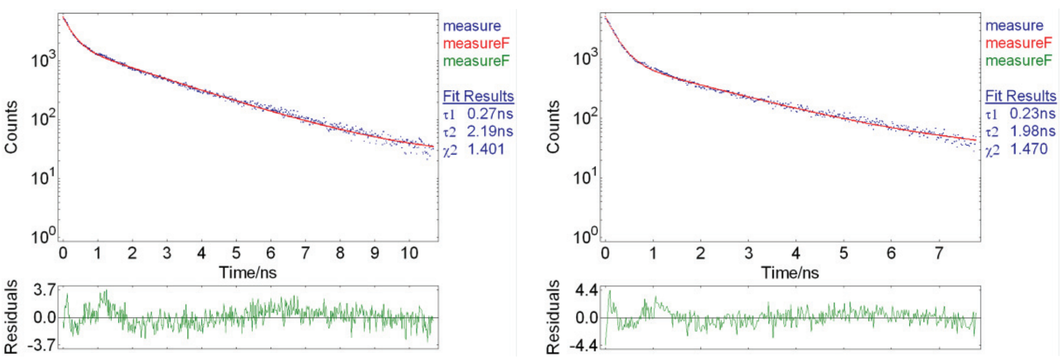

A B

Fig. S18 Radiative decay curves of **4-MeB** in 1,4-dioxane (2.0×10^{-5} mol·L^{-1}) excited at 377 nm: (A) emission at 410 nm; (B) emission at 440 nm.

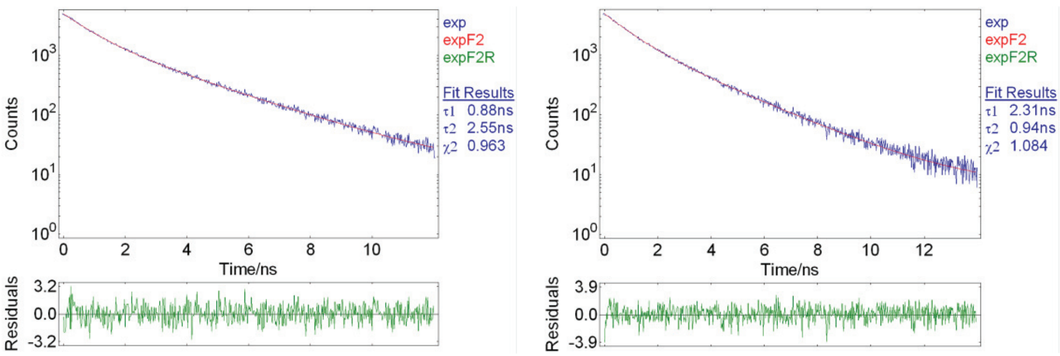

A B

Fig. S19 Radiative decay curves of **4-MeB** in EtOAc (2.0×10^{-5} mol·L^{-1}) excited at 377 nm: (A) emission at 410 nm; (B) emission at 450 nm.

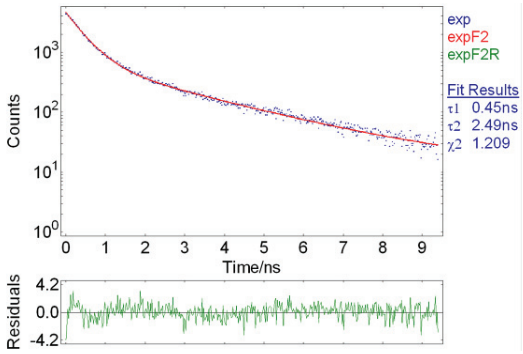

A

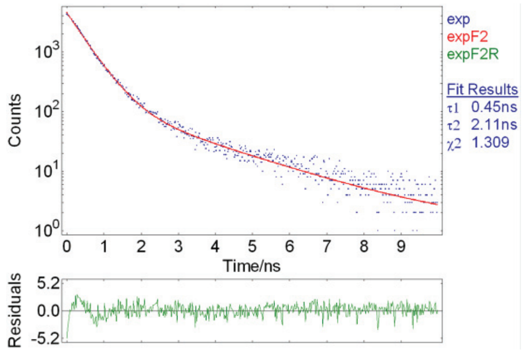

B

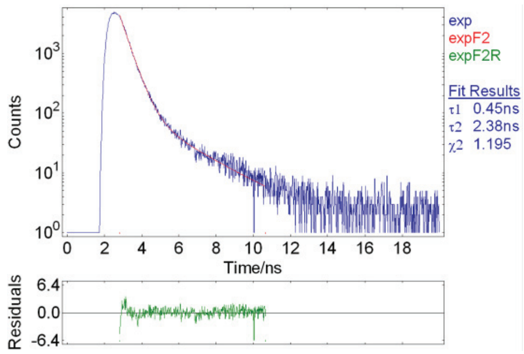

C

Fig. S20 Radiative decay curves of **4-MeB** in THF (2.0×10^{-5} mol·L^{-1}) excited at 377 nm: (A) emission at 410 nm; (B) emission at 450 nm; (C) emission at 490 nm.

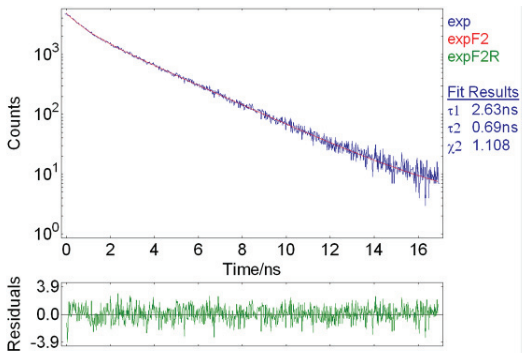

A

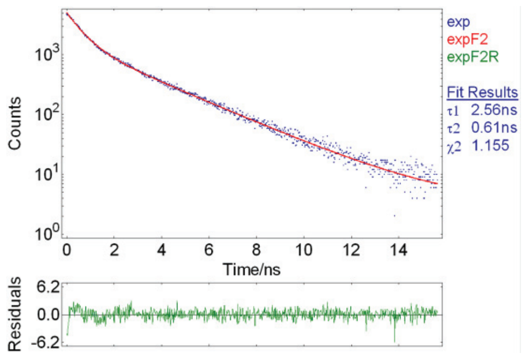

B

Fig. S21 Radiative decay curves of **4-MeB** in DCM (2.0×10^{-5} mol·L^{-1}) excited at 377 nm: (A) emission at 410 nm; (B) emission at 440 nm.

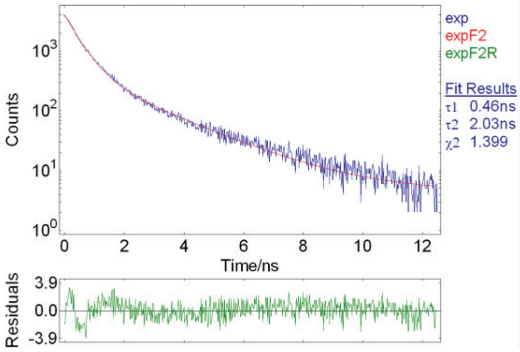

A

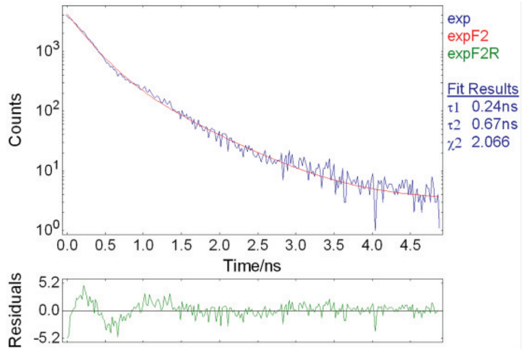

B

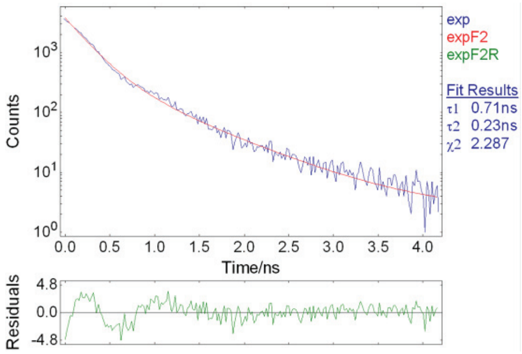

C

Fig. S22 Radiative decay curves of **4-MeB** in methanol (2.0×10^{-5} mol·L^{-1}) excited at 377 nm: (A) emission at 410 nm; (B) emission at 450 nm; (C) emission at 490 nm.

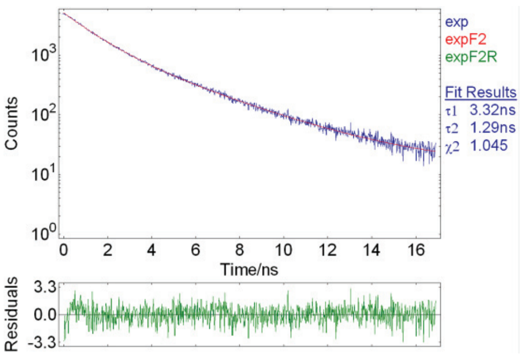

A

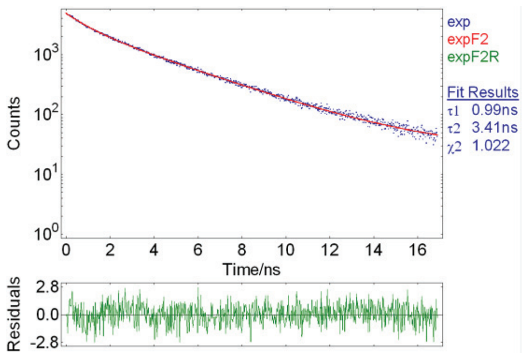

B

Fig. S23 Radiative decay curves of **4-MeB** in DMF (2.0×10^{-5} mol·L^{-1}) excited at 377 nm: (A) emission at 400 nm; (B) emission at 450 nm.

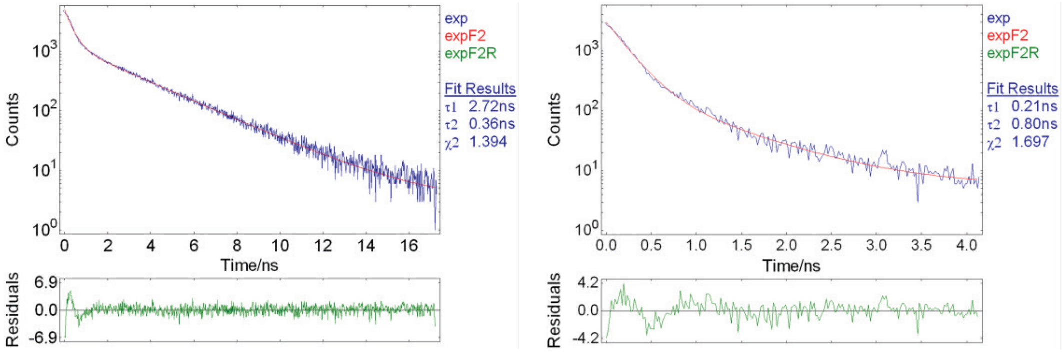

A **B**

Fig. S24 Radiative decay curves of **4-MeB** in acetonitrile (2.0×10^{-5} mol·L^{-1}) excited at 377 nm: (A) emission at 410 nm; (B) emission at 490 nm.

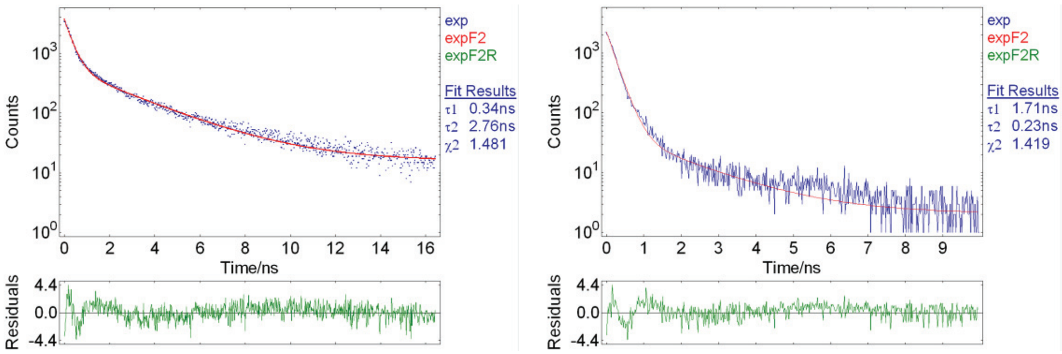

A **B**

Fig. S25 Radiative decay curves of **4-MeB** in DMSO (2.0×10^{-5} mol·L^{-1}) excited at 377 nm: (A) emission at 410 nm; (B) emission at 460 nm.

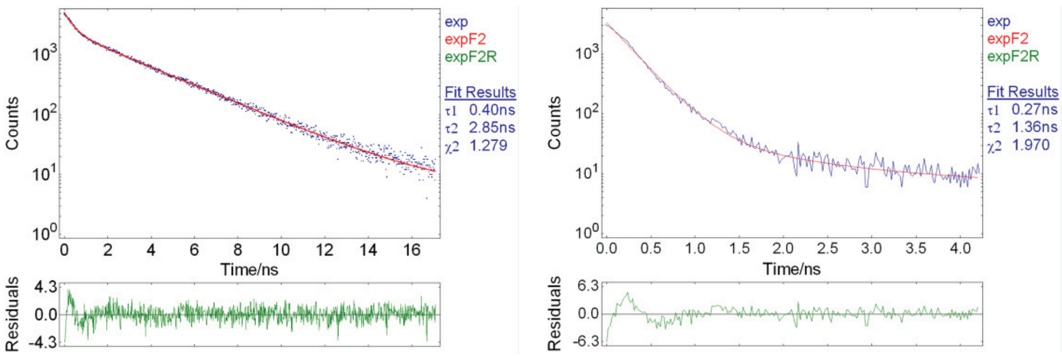

A **B**

Fig. S26 Radiative decay curves of **4-MeB** in water (2.0×10^{-5} mol·L^{-1}) excited at 377 nm: (A) emission at 400 nm; (B) emission at 450 nm.

5. Fluorescence lifetimes

Table S1 The ratio of the fraction of longer-time component to that of the shorter-time in 1,4-dioxne.

λ_{em} /nm	*Lifetimes* / ns		*Relative weights* / %
	τ1	τ2	τ1: τ2
410	2.19	0.27	79.14:20.86
440	1.98	0.23	63.7:36.30

Table S2 The ratio of the fraction of longer-time component to that of the shorter-time in EtOAc.

λ_{em} /nm	*Lifetimes* / ns		*Relative weights* / %
	τ1	τ2	τ1: τ2
410	2.55	0.88	67.28:32.72
450	2.31	0.94	63.5:36.5

Table S3 The ratio of the fraction of longer-time component to that of the shorter-time in THF.

λ_{em} /nm	*Lifetimes* / ns		*Relative weights* / %
	τ1	τ2	τ1: τ2
410	2.49	0.45	49.11:50.89
450	2.11	0.45	15.47:84.53
490	2.38	0.45	13.37:86.63

Table S4 The ratio of the fraction of longer-time component to that of the shorter-time in DCM.

λ_{em} /nm	*Lifetimes* / ns		*Relative weights* / %
	τ1	τ2	τ1: τ2
410	2.63	0.69	85.31:14.69
440	2.56	0.61	66.27:33.73

Table S5 The ratio of the fraction of longer-time component to that of the shorter-time in methanol.

λ_{em} / nm	*Lifetimes* / ns		*Relative weights* / %
	τ1	τ2	τ1:τ2
410	0.46	0.20	63.14:36.86
450	0.67	0.24	35.25:64.75
490	0.71	0.23	32.03:67.97

Table S6 The ratio of the fraction of longer-time component to that of the shorter-time in DMF.

λ_{em} / nm	*Lifetimes* / ns		*Relative weights* / %
	$\tau 1$	$\tau 2$	$\tau 1:\tau 2$
400	3.32	1.29	55.12:44.88
450	3.41	0.99	84.57:15.43

Table S7 The ratio of the fraction of longer-time component to that of the shorter-time in acetonitrile.

λ_{em} /nm	*Lifetimes* / ns		*Relative weights* / %
	$\tau 1$	$\tau 2$	$\tau 1:\tau 2$
410	2.72	0.36	72.07:27.93
490	0.80	0.21	25.08:74.92

Table S8 The ratio of the fraction of longer-time component to that of the shorter-time in DMSO.

λ_{em} /nm	*Lifetimes* / ns		*Relative weights* / %
	$\tau 1$	$\tau 2$	$\tau 1:\tau 2$
410	2.76	0.34	57.61:42.39
460	1.71	0.23	13.02:86.98

Table S9 The ratio of the fraction of longer-time component to that of the shorter-time in H_2O.

λ_{em} /nm	*Lifetimes* / ns		*Relative weights* / %
	$\tau 1$	$\tau 2$	$\tau 1:\tau 2$
400	2.85	0.40	86.90:13.10
450	1.36	0.27	7.01:92.99